**ACS Sustainable Chemistry and Engineering** 3(12) : 3382–3387 (2015) © 2015 American Chemical Society after peer review and technical editing by the publisher. To access the final edited and published work see https://doi.org/10.1021/acssuschemeng.5b01094.

# TAILORING MECHANICAL PROPERTIES OF RIGID POLYURETHANE FOAMS BY SORBITOL AND CORN DERIVED BIOPOLYOL MIXTURES

Lorena Ugarte [†], Sandra Gómez-Fernández [†], Cristina Peña-Rodriguez [†], Aleksander Prociak [‡], Maria Angeles Corcuera [†], Arantxa Eceiza[*,†].

[†] "Materials + Technologies" Research Group (GMT), Department of Chemical and Environmental Engineering, Polytechnic School, University of the Basque Country (UPV/EHU), 20018 Donostia-San Sebastián, Spain

[‡] Department of Chemistry and Technology of Polymers, Cracow University of Technology, Warszawska 24, 31-155 Cracow, Poland

[*]Corresponding autor. E-mail: arantxa.eceiza@ehu.es

ABSTRACT

Sorbitol arises to be a strong candidate for renewably sourced polyol synthesis. Moreover, processes for extracting sorbitol directly from cellulosic materials are showing to be effective and materials such as agroforestry residues could be used as green sorbitol sources. Rigid polyurethane foams were successfully synthesized by using mixtures of a sorbitol based high functionality polyol and a corn based diol. Microstructure and properties of the rigid polyurethane foams were characterized by scanning electron microscopy, Fourier transform infrared spectroscopy, thermogravimetric analysis, thermal conductivity measurements, compression tests, and dynamic mechanical analysis. Results show that the crosslinking density of the formed polymer network was directly modified by polyol mixture ratio and microstructure and properties also changed in consonance. The incorporation of different amounts of a diol with longer chain length between hydroxyl groups allowed fixing the rigidity of the foams, opening the door to the possibility of designing rigid polyurethane foams with tailored properties.

Keywords: rigid polyurethane foam, sorbitol based polyol, corn sugar based polyol, mechanical properties, crosslinking density.

TOC /Abstract art

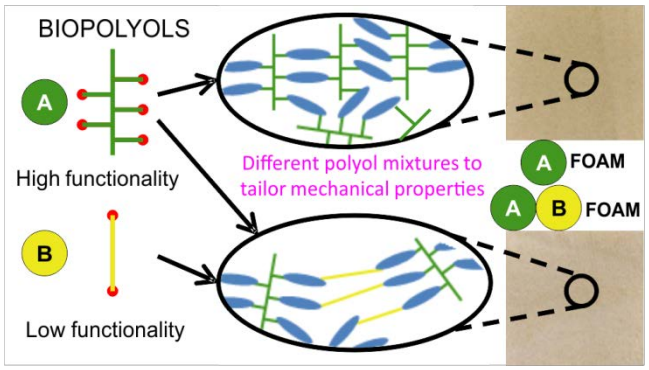


Synopsis: Rigid polyurethane foams with sorbitol and corn based polyols were synthesized and characterized and the possibility of adjusting mechanical properties was analyzed.

## INTRODUCTION

Polyurethanes constitute a large family of polymers which is characterized for their versatility. Depending on the nature of initial reactants, polyurethanes can be synthesized as thermoplastics, adhesives and sealants, coatings or rigid and flexible foams having in common the urethane bond repeated in their structure. Rigid polyurethane foams are widely used in applications such as acoustic and thermal insulation or as lightweight core material in sandwich structures.

The versatility of polyurethanes makes their demand to grow worldwide. New emerging economies are believed to keep this tendency in coming years. Related to this, the environmental impact caused by polyurethane synthesis, use and disposal phases is to be taken into account. Regarding synthesis process, efforts are being made to diminish the use of petroleum derived precursors. Considering that polyol components usually constitute near half the weight of the reacting mixture, using greener polyols in polyurethanes synthesis have attracted much interest in recent years.

Considering both economical and environmental issues, sugar alcohols have gained much interest due to their abundance, availability and renewability. Among them, sorbitol is one of the most popular due to its versatility and applications in many fields such as biomedicine and pharmacy,[1-4] food industry,[5] food packaging is an important operation in food industry,[6,7] cryopreservation,[8] electrochemistry,[9,10] bio-fuels[11] and detergency.[12] Moreover, sorbitol derived polyols can also be used in rigid polyurethane foam synthesis.[13,14]

Sorbitol can be extracted from biomass resources. Although it has traditionally been obtained from corn or wheat starch, nowadays cellulosic biomass products such as agroforestry residues constitute a promising sorbitol resource since they do not compete with the food chain as starch does, they are widely available and it allows waste revaluation. Recent works are focused on the extraction of sorbitol directly from cellulose by a combination of hydrolysis and hydrogenation reactions using heterogeneous catalysts[15-18] including processes in which there is no need of cellulose pre-treatment with acids to reduce its crystallinity.[19] Obtained satisfactory results show that agroforestry residues have great potential as raw materials for sorbitol extraction, being a promising source of green polyols for polyurethane industry.

Sorbitol based polyols have multiple secondary hydroxyl groups, thus very rigid foams with high cross-linking density are obtained. In a previous work concerning rigid polyurethane foams based on renewable polyols, a short modifier with functionality higher than two was incorporated in the formulation with the aim of conferring rigidity to the foam.[20] In this case different amounts of a diol, with higher equivalent weight than the sorbitol based polyol, were incorporated in the formulation in order to modify properties and obtain foams with different grades of rigidity.

In this work, rigid polyurethane foams were synthesized using mixtures of a sorbitol-derived high functionality polyol and a corn sucrose-derived diol, in a one step process using open molds. The effect of polyol mixture ratio over foam morphology and properties was analyzed by the following characterization techniques: scanning electron microscopy (SEM), Fourier transform infrared spectroscopy (FTIR), thermogravimetric analysis (TGA) and thermal conductivity, mechanical testing and dynamic mechanical analysis (DMA).

## EXPERIMENTAL

Rigid polyurethane foams were synthesized by mixtures of sorbitol based Lupranol® 3423 polyether polyol (P440), kindly supplied by BASF, and polytrimethylene ether glycol (P80) obtained from corn sucrose.[21] Polyol properties are summarized in Table 1. Amine catalyst Tegoamin® B75 (Evonik), dibutyltin dilaurate (DBTDL) (Aldrich), surfactant Tegostab® 8404 (Evonik), polymeric 4,4'-diphenylmethane diisocyanate Desmodur® 44V20L (pMDI) (Bayer) and distilled water as blowing agent were also used in the formulation. Isocyanate index was kept constant (I.I.=105) in all foams. Hydroxyl number

of P440 and P80 were calculated according to ASTM D4774-05 standard. For foam synthesis, all reactants except pMDI were vigorously mixed together for 2 minutes using a mechanic rotor and a high-shear stirrer. Then, pMDI was added and stirred for 10 seconds at the same speed. The reactive mixture was left to rise freely and was cured for 24 hours before demolding.

Maximum P80 substitution was established in 30 wt% over total polyol mixture weight. Higher P80 substitutions led to high shrinkages on the final foam with the fixed formulation.

Foams were named as RX where X indicates the amount of P440 polyol parts per hundred total polyol mixture weight. Foams designation, formulation and apparent density values are summarized in Table 2. All formulations are based on parts per hundred polyol (pphp).

*Cell morphology and density*

Cell morphology was analyzed in both perpendicular and parallel surfaces to the foam rise direction by scanning electron microscopy (SEM) by a JEOL-JSM-6400 equipment operated at 20kV with beam currents comprised between 0.05 and 1 nA. Prior to analysis, the samples were gold coated. Apparent core density values of foams were determined according to ASTM D1622-03 standard.

*Reaction kinetics*

Reaction kinetics of foams was evaluated by analyzing the cream time, gel time and tack free time. These characteristic times were measured during the synthesis of the foams using a digital stopwatch.

*Fourier transform infrared spectroscopy*

Attenuated total reflectance infrared (ATR-FTIR) spectroscopy was used to identify the characteristic functional groups of the rigid polyurethane foams. Measurements were performed with a Nicolet Nexus FTIR spectrometer equipped with a MKII Golden Gate accessory, Specac, with diamond crystal as ATR element at a nominal incidence angle of 45º with a ZnSe lens. Single-beam spectra of the samples were obtained after averaging 64 scans in the range from 4000 to 800 $cm^{-1}$ with a resolution of 4 $cm^{-1}$. All spectra were obtained in the transmittance mode.

*Thermogravimetric analysis*

Thermogravimetric analysis was performed on a TGA/SDTA 851 Metler Toledo equipment to evaluate differences on thermal degradation behavior of synthesized polyurethane foams. Samples were heated from room temperature to 650 °C at a heating rate of 10 °C $min^{-1}$ under a nitrogen atmosphere. Samples of 2-3 mg were analyzed. As indicative of the starting of thermal degradation, 5% Weight Loss value was taken.

*Thermal conductivity test*

The thermal conductivity factors (λ) were determined using a Laser Comp Heat Flow Instrument Fox 200. The measurements were made at an average temperature of 10 °C (temperature of cold plate 0 °C and warm plate 20 °C). One specimen was analyzed per sample in the parallel direction to cell growth.

*Mechanical properties*

Compressive properties of foams were evaluated in a MTS equipment with a load cell of 10 kN. Rectangular samples of 20 mm sides x 10 mm height were compressed at room temperature at a crosshead speed of 5 mm $min^{-1}$ until 90% strain was reached. The compressive force was applied in the foam rise direction. The modulus of elasticity and compressive strength were calculated according to ASTM D1621 standard. The densification strain was calculated as the intersection point between the stress plateau and the extrapolation of densification line. To evaluate the recovery values of foams, thickness was measured after 10 minutes and after 24 hours of the compressive test. Recovery values were calculated as shown in Equation 1:

$$R = \frac{t_f - t_0}{t_0} x100 \qquad \text{(Eq. 1)}$$

where R is the recovery at the corresponding recovery time (%), $t_f$ is the thickness measured after the corresponding recovery time (mm) and $t_0$ is the thickness measured just after the compressive test (mm).

All properties were averaged for at least three specimens.

*Dynamic mechanical analysis*

DMA was performed in tensile mode with an Eplexor 100 N analyzer, Gabo equipment. Measurements were carried out at a scanning rate of 2 ºC $min^{-1}$ from -100 to 200 ºC, using an initial strain of 2%. The operating frequency was 1 Hz. Approximate dimensions of foams were 20 x 5.5 x 3.5 $mm^3$ (length x width x thickness).

## RESULTS AND DISCUSSION

Density values of foams are summarized in Table 2. Values diminished as P80 was incorporated in the formulation. An increase on blowing efficiency was observed as P80 content increased. On the same fashion, the required isocyanate quantity diminished and so did the formation of allophanate crosslinks, which hinder foaming reactions.[22] Moreover, the decrease of hydroxyl value is believed to favor bubble coalescence since cell wall elasticity decreased.

SEM images of polyurethane foams are shown in Figure 1. Typical rigid polyurethane foam structure is observed, with closed cells of polygonal shape. SEM images of foams regarding perpendicular surface to the rise direction showed similar cell structures for all foams. However, analyzing SEM images on the parallel surface, it was clearly observed that as P80 quantity increased anisotropy increased. Cells become extended in the foam rise direction and the volume occupied by each cell increased. This phenomenon may be directly related to the increased blowing efficiency previously mentioned. Foam R70 seemed to have the most irregular cell size distribution. Cell size of foams was in accordance with density values.

Table 3 shows the characteristic times measured during foaming reaction. Cream time is defined as the point where bubble rise starts and the color of the mixture changes from dark brown to cream. Gel time corresponds to stable network formation at the end of rising. At the tack free time, the outer surface of the foam loses the stickiness and can be removed from the mold. It was observed that P80 incorporation shortened the characteristics times, that is, reaction rate was increased. The longest times were measured for R100 foam, while the shortest ones were measured for R70. The higher reactivity of primary hydroxyl groups, present on P80 polyol, might be the main factor.[23,24] On the contrary P440 contains only secondary hydroxyl groups which are not so reactive. Ghoreishi et al. modeled the reactivity of polyols depending on the primary or secondary nature of hydroxyl groups.[25] They obtained satisfactory results by

considering the reactivity of primary hydroxyl groups three times higher than the reactivity of secondary hydroxyl groups.

The infrared spectra obtained for rigid polyurethane foam series is shown in Figure 2. They all showed typical polyurethane foam spectra which confirmed that urethane bonds were formed during reaction.[23,26] In fact, stretching bands corresponding to N-H group (3307 $cm^{-1}$), $CH_2$ group (2870 $cm^{-1}$), urethane C=O group (1705 $cm^{-1}$) and C-O group (1072 $cm^{-1}$) were observed. Moreover, N-H plane bending vibration (1540 $cm^{-1}$) and C-N group vibration (1221 $cm^{-1}$) were observed. As both polyols were of polyether nature, no significant changes were observed concerning vibration of polyol characteristic groups. The influence of P80 incorporation was evaluated by analyzing signal intensities in carbonyl stretching region. It was observed that the intensity diminished as higher was the P2 content in the foam, in good agreement with the decrease of urethane linkages due to the decrease of crosslinking density of the foam.

In thermogravimetric analysis of rigid polyurethane foams, shown in Figure 3, one major peak was identified. The minor peak reported in some works[27,28] corresponding mainly to water evaporation at around 110-190 ºC was not observed. Regarding the beginning of thermal degradation at 5% weight loss value in TGA curve (Figure 3, inset), it was observed that the resistance to thermal degradation was directly proportional to P440 content since its higher hydroxyl number formed a more crosslinked structure with more urethane bonds, and higher activation energies were needed for thermal decomposition. Observing the DTGA curve, the heterogeneity of the polyol mixture was evidenced by the width of the degradation peaks, thus R100 foam showed the narrowest peak at 333.5 ºC since it was composed only by P440 polyol. The peak widened as P80 was incorporated in the formulation; in fact, a shoulder was observed in the case of R70 foam. The maximum degradation rate shifted to lower temperatures as the crosslinking density of the foam decreased by P80 incorporation, although the corresponding mass loss lowered probably because of the lower urethane content. Regarding final char content, foams with the highest pMDI and P440 content in the formulation yielded higher char residues due to the higher aromatic content in the polymer backbone.[29,30] The same conclusion was reached in a previous work concerning rigid polyurethane foams. [20]

Thermal conductivity in foams is determined by the conductivity of the polymer phase, conductivity of the gas phase and thermal radiation.[31] Conduction in the gaseous phase

accounts for 65-80% of the overall heat transference, while conduction in the solid phase and radiative transference account for 35-20%.[32] Each mechanism depends mainly on the factors listed next.[33] The gaseous conduction depends on the employed blowing gas; in this case it was the same in all foams. Radiative heat transfer depends on cell size; as lower is the cell size more walls are present which inhibit radiation. The solid conduction on the foam depends on density; as density decreases lower is the solid material quantity by where the heat is transported. Measured thermal conductivity factors (λ) are summarized in Table 5. Values were in the range of those reported in literature.[34-36] Similar conductivity factor values were observed despite the considerable lower density of P80 containing foams. Different densities should affect mainly on the conduction through the solid phase, and thermal conductivity values were expected to decrease as P80 was incorporated. The observed behavior could be due to the tortuosity of the polymer path along the analyzed direction.[37] Although lower density foams present less material for the heat to transfer, according to SEM images their cells are extended in the analyzed direction, and the tortuosity of the path is diminished making easier the heat transference. Therefore, it could be said that the density reduction effect is compensated by the more straightforward path across the polymer matrix in R90, R80 and R70 foams. Additionally, the lower cell size observed in R100 foam may had contributed to a reduction in radiative transference.

Compressive stress-strain curves of foams are shown in Figure 4. It is observed that the elastic modulus and stress values for a given strain are higher for foams with higher P440 polyol content. It is reported in literature that both elastic modulus and compressive strength have a direct relationship with foam density.[38] Foam with higher cell size may have thinner cell walls and hence compressive properties might be affected. To avoid the effect of density, specific properties were analyzed. Specific compression properties of polyurethane foams are summarized in Table 6.

Regarding the results in Table 6, it is observed that specific elastic modulus and compressive strength were influenced by P440 and P80 mixture ratio since their values diminished as P80 quantity increased. Deviation values for specific elastic modulus values were comprised between 0.02 kPa $kg^{-1}$ $m^3$ and 0.01 kPa $kg^{-1}$ $m^3$ whereas deviation values for specific compressive strength were in the range of $10^{-3}$ kPa $kg^{-1}$ $m^3$. A comparison was done between compressive behavior of synthesized rigid polyurethane foams and rigid polyurethane foams obtained from petrochemical polyols with similar

formulation and where water was used as the blowing agent.[39-41] It was observed that compressive mechanical properties were very similar in all cases, considering the mechanical behavior very satisfactory. The introduction of P80 in the formulation implied having longer polyol chains in the foam network and lower crosslinking density. Moreover, the consequent lower isocyanate groups introduced in the formulation diminished the quantity of rigid urethane covalent bonds present in the polymer network.[42] Densification strain values were in the range of 68-82% with deviation values in the range of 1%. As foams were more rigid, densification values diminished indicating that cell walls collapsed and came in contact at lower deformations. Foam density seemed to have a direct relationship with the densification phenomenon,[43] where higher foam densities and hence lower cell sizes implied lower densification values. On the same fashion, as the stiffness of the polymer network diminished higher recovery values were reached both after 10 minutes and after 24 hours.

DMA analysis was used to observe the evolution of storage modulus (E`) and tan δ values with temperature (Figure 5). Although dynamic mechanical properties were analyzed in tensile mode, results showed that they followed the same tendency as the compressive properties did.

The glass transition temperature of the foams can be defined as the maximum of tan δ curve.[44] It could be observed that P80 incorporation led to a decrease of glass transition temperature of the foams (143.5 ºC, 142.4 ºC, 140.5 ºC and 135.8 ªC for R100, R90, R80 and R70 foams, respectively) due to the increase of mobility that longer chains of P80 conferred to the covalent network and because of the lowering of crosslinking density of the foam. As polyol mixture heterogeneity increased, a broadening of the tan δ peak was also observed.[45] Regarding E' values, R100 foam showed the highest values along all temperature range. With respect to foams with P80 polyol E' values were lowered linearly with P80 incorporation. A small drop on E' curve was observed at around 10 ºC, being higher as P80 quantity increased. That could be related with the beginning of molecular motion of P80.[21] Once the glass transition temperature was reached, an abrupt lowering for E' values occurred in all foams.

## CONCLUSIONS

Rigid polyurethane foams were successfully synthesized by sorbitol and corn sourced polyols. In fact, rigid polyurethane foams with polyol mixtures ranging from 100%

sorbitol based P440 polyol to 70% P440 polyol and 30% corn based P80 polyol were obtained. Foams presented a closed-cell structure with different cell shapes depending on whether they were perpendicularly or parallel observed to the rise direction, with lower cell sizes and higher densities for foams with higher P440 quantity. Regarding reaction rate, it was concluded that the reactivity of hydroxyl groups was the most influencing factor, being faster when the polyol with primary hydroxyl groups was incorporated. The decreased crosslinking density and fewer urethane groups due to the lower hydroxyl value of P80 polyol directly influenced the mechanical properties of the foams, which showed comparable values to petrochemical polyol based rigid foams. As the crosslinking density decreased, foams with lower elastic modulus and compressive strength but higher densification strain and recovery values were obtained. Foams with higher crosslinking density showed higher resistance to thermal degradation. Thermal conductivity values were in the range of other natural polyol based rigid foams. Moreover, it was observed that the modification of polyol mixture to tailor mechanical properties will not sacrifice thermal isolation capacity of the foams.

ACKNOWLEDGEMENTS

Financial support from the Basque Government in the frame of Grupos Consolidados (IT-776-13) and from European Union-FP7-PIRSES-GA-2012-BIOPURFIL program is gratefully acknowledged. Additionally, the author thanks the Universty of the Basque Country (UPV/EHU) for funding this work (PIFUPV047/2011). Technical support provided by SGIker (UPV/EHU, MINECO, GV/EJ, ESF) is gratefully acknowledged.

REFERENCES

(1) Schmitt, H.; Creton, N.; Prashanta, K.; Soulestin, J.; Lacrampe, M.-F.; Krawczak, P. Preparation and characterization of plasticized starch/halloysite porous nanocomposites possibly suitable for biomedical applications. *J. Appl. Polym. Sci.* **2015**, *132*, 41341/1-41341/9.

(2) Barret, D. G.; Merkel, T. J.; Luft, J. C.; Yousaf, M. N. One-step syntheses of photocurable polyesters based on a renewable resource. *Macromolecules* **2010**, *43*, 9660-9667.

(3) Teng, L.; Nie, W.; Zhou, Y.; Song, L.; Chen, P. Synthesis and characterization of star-shaped PLLA with sorbitol as core and its microspheres application in controlled drug release. *J. Appl. Polym. Sci.* **2015**, *132*, 42213/1-42213/7.

(4) Pensak, J.; Odile, C.; Warintorn, R. Scavenging activity of rutin encapsulated in low methoxyl pectin beads. *Cell. Chem. Technol.* **2015**, *49*, 51-54.

(5) Malgorzata, G. Sugar alcohols-their role in the modern world of sweeteners: a review. *Eur. Food Res. Technol.* **2015**, *241*, 1-14.

(6) Wagh, Y. R.; Pushpadass, H. A.; Emeral, F. M. E.; Nath, B. S. Preparation and characterization of milk protein films and their application for packaging of Cheddar cheese. *J. Food Sci. Technol*. **2014**, *51*, 3767-3775.

(7) Hong, S.-I.; Lee, J.-W.; Son, S.-M. Properties of polysaccharide coated polypropylene films as affected by biopolymer and plasticizer types. *Packag. Technol. Sci.* **2005**, *18*, 1-19.

(8) Ivanisenko, N. V.; Dzuba, S. A. Molecular motion in frozen phospholipid bilayers in the presence of sucrose and sorbitol studied by the spin-echo EPR of spin labels. *Appl Magn. Reson*. **2013**, *44*, 883-891.

(9) de Almeida, M. R. H.; Barbano, E. P.; Carvalho, M. F.; Tulio, P. C.; Carlos, I. A. Copper-zinc electrodeposition in alkaline-sorbitol medium: Electrochemical studies and structural, morphological and chemical composition characterization. *Appl. Surf. Sci.* **2015**, *333*, 13-22.

(10) Hamid, Z. A.; Aal, A. A. New environmentally friendly noncyanide alkaline electrolyte for copper electroplating. *Surf. Coat. Tech.* **2009**, *203*, 1360-1365.

(11) Zhang, Q.; Wang, T.; Li, B.; Jiang, T.; Ma, L.; Zhang, X.; Liu, Q. Aqueous phase reforming of sorbitol to bio-gasoline over Ni/HZSM-5 catalyst. *Appl. Energ.* **2012**, *97*, 509-513.

(12) Dontulwar, J. R.; Borikar, D. K. Synthesis of green liquid detergents using carbohydrate polymers based on white dextrin, sorbitol and maleic anhydride. *Asian J. Chem.* **2011**, *23*, 2511-2514.

(13) Ionescu, M. Chemistry and Technology of polyols for polyurethanes; iSmithers Rapra Publishing: Shrewsbury, U.K., 2005.

(14) Desroches, M., Escouvois, M., Auvergne, R., Caillol, S., & Boutevin, B. From vegetable oils to polyurethanes: synthetic routes to polyols and main industrial products. *Polymer Reviews*. **2012**, *52*(1), 38-79.

(15) Zhang, J.; Li, J.; Wu, S.-B.; Liu, Y. Advances in the catalytic production and utilization of sorbitol. *J. Ind. Eng. Chem.* **2013**, *52*, 11799-11815.

(16) Han, J. W.; Lee, H. Direct conversion of cellulose into sorbitol using dual-functionalized catalysts in neutral aqueous solution. *Catal. Commun.* **2012**, *19*, 115-118.

(17) Shrotri, A.; Tanskale, A.; Beltramini, J. N.; Gurav, H.; Chilukuri, S. V. Conversion of cellulose to polyols over promoted nickel catalysts. *Catal. Sci. Technol.* **2012**, *2*, 1852-1858.

(18) Wang, D.; Niu, W.; Tan, M.; Wu, M.; Zheng, X., Li, Y.; Tsubaki, N. Pt nanocatalysts supported on reduced graphene oxide for selective conversion of cellulose or cellobiose to sorbitol. *ChemSusChem* **2014**, *7*, 1398-1406.

(19) S. Ribeiro, L.; Orfao, J. M.; R. Pereira, M. F. Enhanced direct production of sorbitol by cellulose ball-milling. *Green Chem*. **2015**, *17*, 2973-2980.

(20) Calvo-Correas, T.; Mosiewicki, M. A.; Corcuera, M. A.; Eceiza, A.; Aranguren, M. I. Linseed oil-based polyurethane rigid foams: synthesis and characterization. *J. Renew. Mater.* **2015**, *3*, 3-13.

(21) Ugarte, L.; Fernández-d'Arlas, B.; Valea, A.; Gonzalez, M. L.; Corcuera, M. A.; Eceiza, A. Morphology–properties relationship in high renewable content polyurethanes. *Polym. Eng. Sci*. **2014,** *54*, 2282–2291.

(22) Ho, L.; Sung, H. K.; Byung, K. K. Effect *of hydroxyl value of polyol in rigid polyurethane foams. Polym. Adv. Technol.* **2008**, *19*, 1729-1734.

(23) Septevani, A. A.; Evans, D. A. C.; Chaleat, C.; Martin, D. J.; Annmalai, P. K. A systematic study substituting polyether polyol with palm kernel oil based polyester polyol in rigid polyurethane foam. *Ind. Crop. Prod.* **2015**, *66*, 16-26.

(24) Hu, Y. H.; Gao, Y.; Wang, D. N.; Hu, C. P.; Zu, S.; Vanoverloop, L. Randall, D. Rigid polyurethane foam prepared from rapeseed oil based polyol. *J. Appl. Polym. Sci.* **2002**, *84*, 591-597.

(25) Goreishi, R.; Zhao, Y.; Suppes, G. J. Reaction modeling of urethane polyols using fraction primary, secondary and hindered secondary hydroxyl contents. *J. Appl. Polym. Sci.* **2014**, 131, 40388/1-40388/6

(26) Abdel Hakim, A. A.; Nassar, M.; Emam, A.; Sultan, M. Preparation and characterization of rigid polyurethane foams prepared from sugar-cane bagasse polyol. *Mater. Chem. Phys.* **2011**, *129*, 301-307.

(27) Jiao, L.; Xiao, H.; Wang, Q.; Sun, J. Thermal degradation characteristics of rigid polyurethane foam and the volatile products analysis with TG-GTIR-MS. *Polym. Degrad. Stab.* **2013**, *98*, 2687-2696.

(28) Sing, H.; Sharma, T. P.; Jain, A.K. Reactivity of the raw materials and their effects on the structure and properties of rigid polyurethane foams. *J. Appl. Polym. Sci.* **2007**, 106, 1014-1023

(29) Einhorn, I. N.; Mickelson, R. W. Char formation in rigid urethane foam. *Papers presented at [the] Meeting - American Chemical Society, Division of Organic Coatings and Plastics Chemistry* **1968**, 28, 291-310

(30) Wang, S.; Chen, H.; Zhang, L. Thermal decomposition kinetics of rigid polyurethane foam and ignition risk by a hot particle. J. Appl. Polym. Sci. **2014**, *131*, 39359/1-39359/9.

(31) Jarfelt U, Ramnas O. Thermal conductivity of polyurethane foam – best performance. In: The 10th International Symposium on District Heating and Cooling, September 3–5; 2006

(32) Lee, S. T.; Scholz, D. P. K. *Polymeric foams: Technology and developments in regulation, process and products; CRC Press: Boca Raton, U.S.A., 2009*

(33) Biedermann, A.; Kukode, C.; Merten, A.; Minogue, E.; Rotermund, U. Heat-transfer mechanisms in polyurethane rigid foam. *High Temp.-High Press.* **2001**, *33*, 699-706.

(34) Cateto, C.; Barreiro, F.; Rodrigues, A.; Belgacem, N. Rigid polyurethane foams from lignin-based polyols. AIP Conference Proceedings **2008**, *1042*, (IVth International Conference on Times of Polymers (TOP) and Composites, 2008), 243-245. Publisher: American Institute of Physics.

(35) Mosiewicki, M. A.; Dell'Arcipetre, G. A.; Aranguren, M. I.; Marcovich, N. E. Polyurethane foams obtained from castor oil-based polyol and filled with wood flour. *J. Compos. Mater.* **2009**, *43*, 3057-3072.

(36) Kacperski, M.; Spychaj, T. Rigid polyurethane foams with poly(ethylene terephthalate)/triethanolamine recycling products. *Polym. Advan. Technol.* **1999**, *10*, 620-624.

(37) Barrios, M. Material characterization of rigid foam insulation for aerospace vehicles. *Electronic theses, treatises and disertations*. Paper 4710, 2011

(38) Tu, Y.-C.; Kiatsimkul, P.; Suppes, G.; Hsieh, F.-H. Physical properties of water-blown rigid polyurethane foams from vegetable oil-based polyols. *J. Appl. Polym. Sci.* **2007**, *105*, 453-459.

(39) Seo, W. J.; Jung, H. C.; Hyun, J. C.; Kim, W. N.; Lee. Y.-B.; Choe, K. H.; Kim, S.-B. Mechanical, Morphological, and Thermal Properties of Rigid Polyurethane Foams Blown by Distilled Water. *J. Appl. Polym. Sci.* **2003**, 90, 12-21

(40) Seo, W. J.; Park, J. H.; Sung, Y. T.; Hwang, D. H.; Kim, W. N.; Lee, H. S. Properties of wáter blowin rigid polyurethane foams with reactivity of raw materials. *J. Appl. Polym. Sci.* **2004**, 93, 2334-2342

(41) Thirumal, M.; Khastgir, D.; Singha, N. K.; Manjunath, B. S.; Naik, Y. P. Effect of a nanoclay on the mechanical, thermal and flame retardant properties of rigid polyurethane foam. *J. Macromol. Sci. Part A* **2009**, 46, 704-712.

(42) Kumar, M.; Kaur, R. Effect of different formulations of MDI on rigid polyurethane foams based on castor oil. *IJSRR*, **2013**, *2*, 29-42.

(43) Courtney, T. H. *Mechanical behavior of Materials: second edition, chapter 14 Cellular Solids*; Waveland Press: Long Grove, U.S.A., 2005.

(44) Gupta, R. K.; Ionescu, M.; Radojcic, D.; Wan, X.; Petrovic, Z. S. Novel renewable polyols based on limonene for rigid polyurethane foams. *J. Polym. Environ.* **2014**, *22*, 304-309.

(45) Suresh, K. I. Rigid polyurethane foams from cardanol: synthesis, structural characterization, and evaluation of polyol and foam properties. *ACS Sustainable Chem. Eng.* **2013**, *1*, 232-242.

TABLES AND FIGURES

**Table 1. Designation, hydroxyl number ($I_{OH}$), position of hydroxyl groups and equivalent weight of the polyols**

| Polyol | Designation | $I_{OH}$ (mg KOH $g^{-1}$) | Position of hydroxyl groups | Equivalent weight (g $eq^{-1}$) |
|---|---|---|---|---|
| Lupranol® 3423 | P440 | 444.2 ± 1.1 | Secondary | 126.2 ± 0.4 |
| Polytrimethylene ether glycol | P80 | 79.4 ± 0.8 | Primary | 706.3 ± 1.1 |

**Table 2. Designation, formulation and apparent density values of synthesized foam series**

| Designation | P440 (pphp*) | P80 (pphp*) | pMDI (pphp*) | $H_2O$ (pphp*) | ρ (kg $m^{-3}$) |
|---|---|---|---|---|---|
| R100 | 100 | - | 54.7 | 1 | 102.56 ± 2.71 |
| R90 | 90 | 10 | 52.8 | 1 | 68.90 ± 3.72 |
| R80 | 80 | 20 | 50.8 | 1 | 66.27 ± 1.71 |
| R70 | 70 | 30 | 48.7 | 1 | 66.03 ± 1.94 |

* pphp: parts per hundred polyol

**Table 3. Cream time, gel time and tack free time of synthesized polyurethane foams**

| | Cream time (s) | Gel time (s) | Tack free time (s) |
|---|---|---|---|
| R100 | 169 | 185 | 190 |
| R90 | 148 | 159 | 171 |
| R80 | 146 | 157 | 165 |
| R70 | 141 | 151 | 153 |

**Table 4. Thermal conductivity factor (λ) values for synthesized rigid polyurethane foams**

| Sample | λ (mW $m^{-1}$ $K^{-1}$) |
|---|---|
| R100 | 35.37 |
| R90 | 35.95 |
| R80 | 36.43 |
| R70 | 36.36 |

**Table 5. Specific modulus of elasticity (E/ρ), specific compressive strength ($\sigma_c/\rho$), densification strain ($\varepsilon_D$), recovery after 10 minutes ($R_{10}$) and recovery after 24 hours ($R_{24}$) of rigid polyurethane foams**

| Foam | E/ρ (kPa $kg^{-1}$ $m^3$) | $\sigma_c/\rho$ (kPa $kg^{-1}$ $m^3$) | $\varepsilon_D$ (%) | $R_{10}$ (%) | $R_{24}$ (%) |
|---|---|---|---|---|---|
| R100 | 9.6 ± 0.0 | 9.9 ± 0.0 | 68.2 ± 2.8 | 3.5 ± 0.4 | 12.9 ± 0.8 |
| R90 | 7.4 ± 0.0 | 9.1 ± 0.0 | 72.5 ± 1.3 | 6.3 ± 0.3 | 15.5 ± 0.7 |
| R80 | 5.9 ± 0.0 | 7.5 ± 0.0 | 75.7 ± 1.8 | 7.9 ± 0.5 | 19.8 ± 1.1 |
| R70 | 3.5 ± 0.0 | 6.0 ± 0.0 | 82.1 ± 1.1 | 10.3 ± 0.5 | 23.7 ± 1.7 |

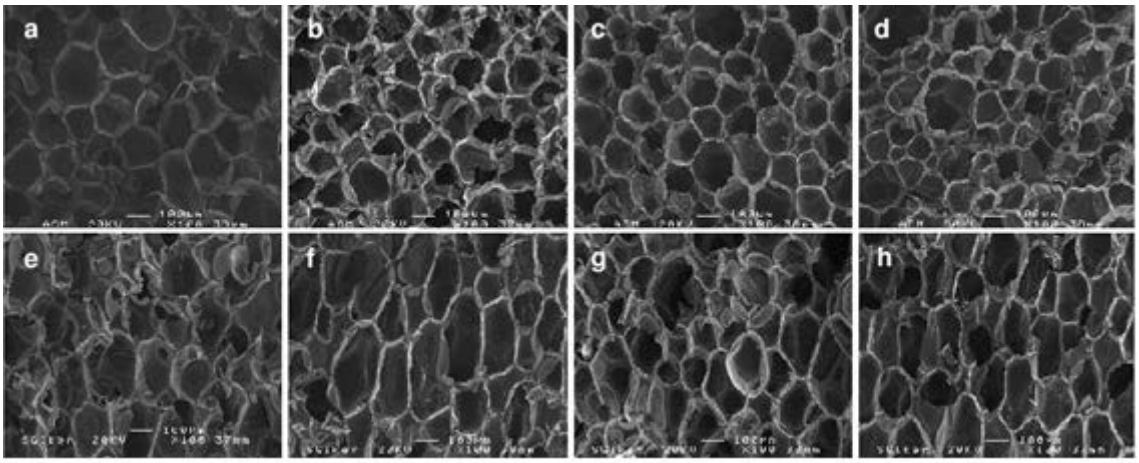


Figure 1. SEM images of (a) R100, (b) R90, (c) R80, (d) R70 perpendicular surface to the rise direction and SEM images of (e) R100, (f) R90, (g) R80, (h) R70 parallel surface to the rise direction. Magnification: 100x.

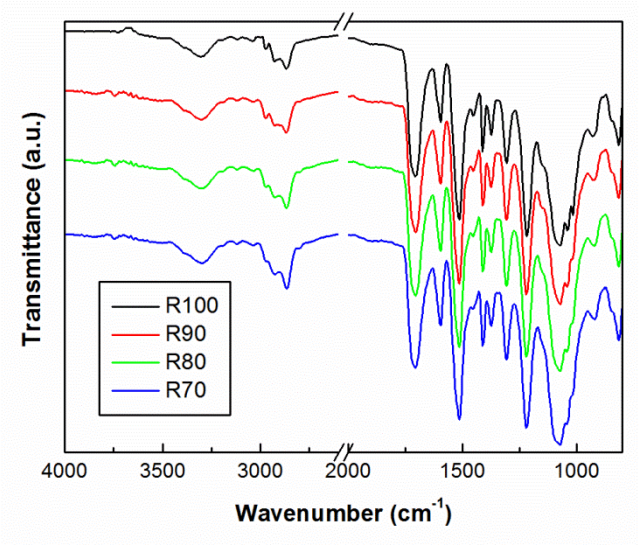


Figure 2. FTIR spectra of rigid polyurethane series.

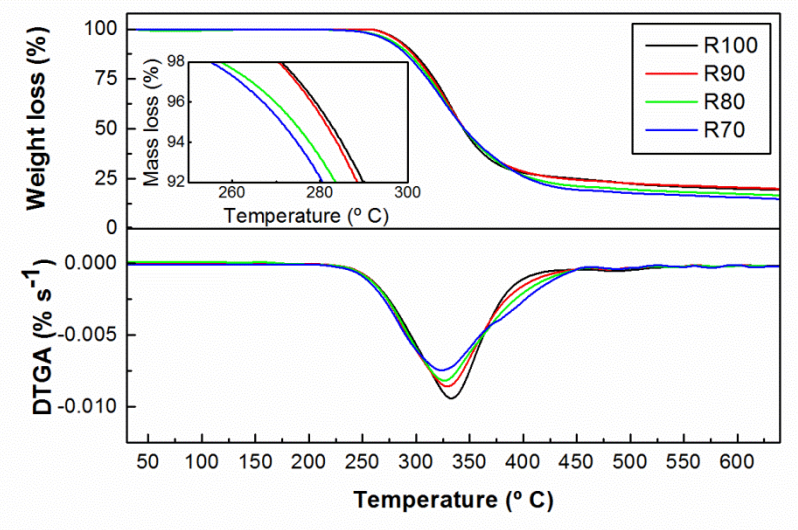


Figure 3. TGA and DTGA curves of synthesized polyurethanes. Inset: magnification of initial degradation stage.

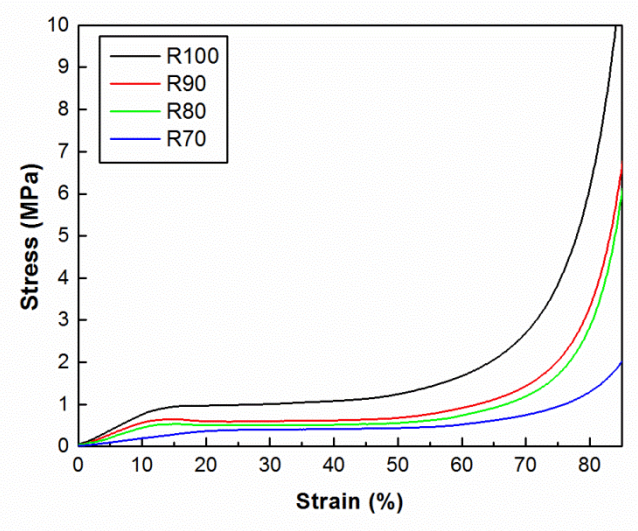


Figure 4. Stress-strain curves in compression mode of the synthesized foams.

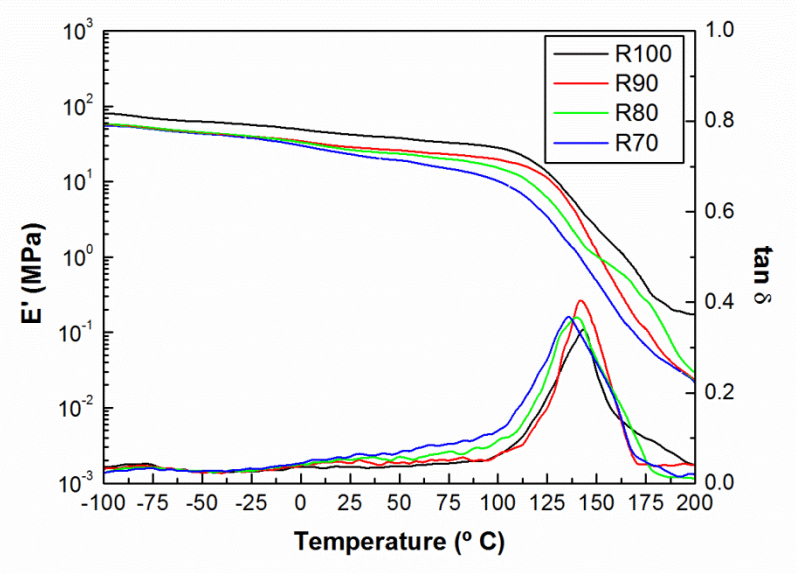


Figure 5. Storage modulus (E') and tanδ values of rigid polyurethane foams.